HIV alters CD4/CXCR4 expression patterns in OP9-DL1-mediated differentiation of human cord-derived CD34^{+} cells

Tetsuo Tsukamoto [1, 2, 3]

[1] The Kirby Institute for infection and immunity in society, University of New South Wales, Sydney, Australia

[2] Center for AIDS Research, Kumamoto University, Kumamoto, Japan

[3] Department of Immunology, Kindai University Faculty of Medicine, Osaka, Japan

Author mailing address: Department of Immunology, Kindai University Faculty of Medicine, 377-2 Onohigashi, Osakasayama-shi, 589-8511 Osaka, Japan

Telephone: +81 72 366 0221

Fax: +81 72 367 7660

Email: ttsukamoto@med.kindai.ac.jp

Abstract

HIV-1 infects and depletes $CD4^+$ T cells, leading to AIDS. The virus is also known to target thymocytes, resulting in decreased T-cell production. On the other hand, the impact of HIV infection upon the dynamics of hematopoietic $CD34^+$ cells is still poorly understood, despite that HIV-positive patients frequently manifest myelosuppression. Here we utilized the OP9-DL1 coculture system that supports in vitro T-lineage differentiation of human $CD34^+$ hematopoietic stem/progenitor cells. Using the system, we established an in vitro model to analyze the differentiation process of human $CD34^+$ cells in the presence of HIV-1. First, we successfully infected cord-derived $CD34^+$ cells with CXCR4-tropic HIV-1_{NL4-3}. HIV-infected cocultures showed sustained HIV replication in both $CD34^+$ and $CD34^-$ cells for 5 weeks, resulting in reduced growth of the whole, $CD4^+CD8^+$ thymocyte, and $CD4^+$ T-cell counts at weeks 3-5. To further understand the dynamics of $CD34^+$ cells, a short coculture assay was performed in which in vitro pre-cocultured cell mixtures were infected with HIV-1_{NL4-3}, cocultured again for 1 week, and analyzed. This resulted in reduced CXCR4 expression in $CD34^+CD7^+$ lymphoid progenitor cells but not in $CD34^+CD7^-$ or $CD34^-$ cells. We also detected possible CD4 upregulation of HIV-infected $CD34^+CD7^+$ cells. These results implicate the possible role of CXCR4-tropic HIV-1 strains in the AIDS pathogenesis by disrupting the $CD34^+CXCR4^+$ cell pools in hematopoiesis and T-lineage differentiation, although the underlining mechanisms remain unclear.

Keywords

human immunodeficiency virus (HIV), acquired immunodeficiency syndrome (AIDS), hematopoietic stem/progenitor cells (HSPC), C-X-C chemokine receptor type 4 (CXCR4)

Introduction

HIV infection is associated with hematological changes (Parinitha and Kulkarni, 2012). Antiretroviral therapy (ART) is effective in the control of viremia and the treatment of AIDS. However, some patients fail to show sufficient T-cell immune restoration despite being aviremic during treatment (Corbeau and Reynes, 2011). HIV-infected patients may show decreased thymopoiesis for generation of new T cells (Blom et al., 2011). Thymic dysfunction occurs during HIV disease and is associated with rapid progression in infants with prenatal HIV infection (Ye et al., 2004). A previous report tested coculture of $CD34^+$ cells and fetal thymic epithelial cells in the presence or absence of HIV-1. This resulted in inhibition of thymocyte maturation at early stages ($CD44^+CD25^-CD3^-$) (Knutsen et al., 1999). Pancytopenia may occur as a result of bone marrow abnormalities in HIV-infected individuals (Alexaki and Wigdahl, 2008; Tripathi et al., 2005). A previous study showed depletion of $CD34^+CD4^+$ cells in bone marrow from HIV-infected patients. However, the study failed to find any evidence for HIV infection of these cells (Banda et al., 1999).

The thymopoiesis environments can be mimicked in vitro by using an OP9-DL1 or OP9-DL4 cell line. These cell lines were derived from the OP9 mouse stromal cell line by transduction with a notch ligand called delta-like 1 or 4 (DL1 or DL4) (Nakano et al., 1994; Schmitt et al., 2004). The OP9-DL1's functions to support thymopoiesis in vitro were first demonstrated in coculture with mouse cells (Nakano et al., 1994). The cell line is also known to support differentiation of human $CD34^+$ hematopoietic stem/progenitor cells (HSPCs) to thymocytes and T cells (De Smedt et al., 2004). There is evidence for production of stromal derived factor-1 (SDF-1, also known as CXCL12),

a ligand for CXCR4, in OP9-DL1 (Janas et al., 2010). Although OP9-DL4 can induce both specific myeloid cells and T-lineage cells, OP9-DL1 only allows differentiation of T-lineage cells while inhibiting B cells and myeloid cells (Mohtashami et al., 2010). Thus, the OP9-DL1 coculture system is used for investigation of the events associated with T-lineage differentiation.

CXCR4 and CCR5 are common coreceptors of HIV-1 (Weiss, 1996). The control of CCR5-tropic strains of HIV-1 is usually considered to be a better correlate of good clinical outcomes than CXCR4-tropic HIV-1 strains (Grivel and Margolis, 1999). This is due to the fact that memory $CD4^+$ T cells express higher levels of CCR5 and are susceptible to CCR5-tropic HIV infection and the following depletion (Schnittman et al., 1990). Because of this, CCR5 may appear to be more closely involved in the immunopathogenesis of the HIV disease than CXCR4 (Okoye and Picker, 2013). On the other hand, the biological functions of CXCR4 has been well documented in biological science fields such as developmental biology and hematology. CXCR4 interacts with SDF-1 and allows CXCR4-expressing cells to home to the loci where SDF-1 is highly expressed (Kucia et al., 2004). The roles of SDF-1 and CXCR4 are essential in human stem cell homing and repopulation of the host with differentiated hematopoietic cells (Kucia et al., 2005; Lapidot and Kollet, 2002). SDF-1 is also produced by thymic epithelial cells and plays an important role in migration of immature progenitors in the thymus (Plotkin et al., 2003).

Therefore, it may be important to better understand the influence of CXCR4-tropic HIV-1 infection upon CXCR4-associated biological events including hematopoiesis and T cell development. There was an attempt to see the impact of CXCR4-tropic simian-human immunodeficiency virus (SHIV) infection on production of T-lineage cells in the thymus of newborn rhesus macaques (Suzuki et al., 2005a). However, it is

not realistic to closely follow the in vivo bone marrow/thymus events in HIV-infected individuals. Instead, humanized mouse models can be beneficial for the purposes (Dudek and Allen, 2013; Marsden et al., 2012). Moreover, an easy-to-use ex-vivo model may be helpful for close monitoring of the differentiation of HSPCs to T-lineage cells in the presence of HIV-1. The present study was aimed at pursuing the in vitro fate of $CD34^+$ progenitor cells and derivatives exposed to HIV-1 using the OP9-DL1 coculture system.

Materials and Methods

Virus stocks. Stocks of HIV-1_{NL4-3} were produced by transfection of the 293T cell line with the molecular clone DNA pNL4-3 (Adachi et al., 1986). After transfection, the culture supernatant was collected and viral loads were determined using an HIV p24 Enzyme-Linked ImmunoSorbent Assay (ELISA) kit (ZeptoMetrix, US).

Cells. Umbilical cord blood samples were collected at Fukuda Hospital, Kumamoto following informed consent. Cord blood mononuclear cells were isolated using Pancoll (PAN-Biotech GmbH, Germany) and by centrifugation at 800 rpm for 20 minutes. $CD34^+$ cells were labeled and selected using human CD34 micro beads and LS columns (Miltenyi Biotec, Japan). The purity was constantly more than 92%. An OP9-DL1 cell line, generated by transduction of the OP9 cell line (ATCC CRL-2749) with human Delta-like 1, was provided by Prof. Seiji Okada (Center for AIDS Research, Kumamoto University, Japan). The cell line was maintained in α-MEM media supplemented with 10% heat inactivated fetal bovine serum (GE Healthcare, Japan).

Antibodies. The following antibodies were used for the flow cytometric analysis of primary cord-derived $CD34^+$ cells and human cells cocultured with OP9-DL1. Anti-human CD8 Brilliant Violet (BV) 510 (clone RPA-T8), anti-human CD3 PE-Cy7 (clone UCHT1), and anti-human CD34 APC (clone 8G12) were purchased from BD Biosciences (Tokyo, Japan). Anti-human CD4 PE-Cy7 (clone OKT4), anti-human CD4 PerCP-Cy5.5 (clone OKT4), and anti-human CXCR4 BV421 (clone 12G5) were purchased from BioLegend (Tokyo, Japan). Anti-human CD3 ECD (clone UCHT1), and anti-HIV-1 p24 PE (clone FH190-1-1, also known as KC57 RD1) were purchased

from Beckman Coulter (Tokyo, Japan). Anti-human CD7 FITC (clone CD7-6B7) was purchased from CALTAG Laboratories (CA, USA),

Coculture of human cells with OP9-DL1. The OP9-DL1 coculture experiment was performed following the previously published protocol with modifications (Holmes and Zuniga-Pflucker, 2009). Briefly, 2×10^5 HIV-infected or uninfected cord-derived $CD34^+$ cells were seeded in a 6-well plate containing a monolayer of OP9-DL1. The coculture was maintained for 5 weeks in the α-MEM media supplemented with 20% heat inactivated FBS, 5 ng/mL recombinant human FMS-like tyrosine kinase 3 ligand (Flt-3L), and 5ng/mL recombinant human interleukin 7 (IL-7). Cells were passaged every week by vigorous pipetting and filtering through a 70-μm membrane, and cocultured again with a fresh monolayer of OP9-DL1. Part of collected cells were analyzed by flow cytometry.

HIV infection. The method for in vitro HIV infection of $CD34^+$ cells was described previously (Tsukamoto and Okada, 2017). For infection of primary cord-derived $CD34^+$ cells with HIV-1_{NL4-3}, a 48-well plate was treated overnight with RetroNectin (Takara Bio Inc., Tokyo, Japan) at a concentration of 10 μg/mL. $CD34^+$ cells were re-suspended in the OP9-DL1 media, seeded at 2×10^5 per well in the coated plate and infected with 200 ng (p24) of HIV-1_{NL4-3} and using spinoculation at 1,200 g, 34 °C for 30 minutes. Cells were further cultured overnight and cocultured in a 6-well plate with a fresh monolayer of OP9-DL1. For HIV infection of OP9-cocultured human cells, the cell concentration was modified to 5×10^5 per well.

Flow cytometric analysis. Surface and intracellular antigen expression was analyzed with FACS LSR II (BD Biosciences), FACS Diva v6.0, and the FlowJo v10.3 (TreeStar). Dead cells were discriminated with Live/Dead Fixable Near-IR Dead Cell Stains (Thermo Fisher Scientific). Live cells were further gated to exclude doublets from the analysis by plotting FSC-W and FSC-A.

PCR analysis of the HIV DNA. Cellular DNA was extracted using Kaneka Easy DNA Extraction Kit (Kaneka, Takasago, Japan). DNA extraction was followed by the PCR analysis using an HIV *gag* primer set (sense: 5'-AGTGGGGGGACATCAAGCAGCCATGCAAAT-3', antisense: 5'-TACTAGTAGTTCCTGCTATGTCACTTCC-3') as described previously (Suzuki et al., 2005b).

Statistical analysis. Statistical analysis was performed using the Graphpad Prism software version 7.0. Statistical significance was defined as $P < 0.05$. Comparison between HIV-infected and uninfected samples was done by Wilcoxon matched-pairs signed rank test, unless otherwise stated. Multiple comparison analyses were done, if necessary, using the Dunn's method. Spearman's correlation coefficiencies were calculated for correlation analyses.

Results

Infection of primary human code-derived CD34$^+$ cells with CXCR4-tropic HIV-1$_{NL4-3}$

Two separate in vitro experiments were performed in the study. The data for the first experiment (long coculture) are shown in Figures 1-3, and S1-3. To follow the in vitro fate of HIV-preexposed CD34$^+$ cells and derivatives for several weeks, we attempted HIV infection of primary human code-derived CD34$^+$ cells. Those cells were confirmed to be partially CD4$^+$ and CXCR4$^+$ after CD34 magnetic bead separation (Fig 1B). The cells were exposed to 200 ng (p24) of HIV-1$_{NL4-3}$. Following centrifugation and overnight incubation, the cells were cocultured with OP9-DL1 (Fig 1A). After a week of coculture, the cells were tested for HIV-1 p24 expression (Fig 1C). Intracellular HIV-1 p24 was detected in both CD34$^+$ and CD34$^-$ cells (Fig 1C). HIV infection was further checked by magnetic bead separation of CD34$^+$ and CD34$^-$ cells followed by DNA extraction and detection of HIV-1 *gag* DNA using PCR (Fig 1D). In this way, the HIV-preexposed cells were prepared for coculture with OP9-DL1.

Persistent HIV-1 infection observed in the OP9-DL1 cocultures with cord-derived CD34$^+$ cells

The above cocultures of HIV-preexposed CD34$^+$ cells and derivatives were maintained for five weeks. All the HIV-infected samples showed persistent HIV-1 p24 expression in 0.1-3.5% of the total cocultured human cells (Fig 1E). Both the HIV-1 p24$^+$ percentages and the cell counts peaked at week 3 (Fig 1E and F). Viral replication levels were further confirmed by measuring HIV-1 p24 amounts in the coculture supernatants using ELISA (Fig 1G). Correlation was found between intracellular HIV-

1 p24$^+$ cell counts and supernatant HIV-1 p24 concentrations by plotting data in Fig 1F and G (Fig 1H).

The dynamics of CD4$^+$ cells in the OP9-DL1 cocultures with HIV-preexposed CD34$^+$ cells

The influence of HIV preexposure of CD34$^+$ cells upon post-coculture events was analyzed by flow cytometry every week until week 5. CD19$^+$, CD20$^+$, or CD33$^+$ cells were not detected in the samples tested (data not shown). HIV-infected cocultures had significantly lower whole cell counts at weeks 3, 4, and 5 post-coculture than uninfected cocultures (Fig 2A). This demonstrates that HIV preexposure of CD34$^+$ cells resulted in impaired cell growth in the cocultures. Similarly, the CD4$^+$CD8$^+$ cell counts were significantly smaller in HIV$^+$ cocultures than HIV$^-$ cocultures (Fig 2B and C). The CD4$^+$CD8$^+$CXCR4$^+$ cell counts showed similar tendencies except that the average CD4$^+$CD8$^+$CXCR4$^+$ cell counts at week 2 was higher in HIV$^+$ than in HIV$^-$ samples (Fig 2D).

Next, the CD34$^-$ cells were gated and analyzed for the expression of CD7 and CD4 (Fig 2E). The CD34$^-$CD7$^+$CD4$^+$ cell counts were not significantly different between HIV-infected and uninfected samples (Fig 2F). It may be noted that HIV$^+$ samples showed higher average CD34$^-$CD7$^+$CXCR4$^+$ cell counts than uninfected samples at weeks 1 and 2 (Fig 2F), as observed with CD4$^+$CD8$^+$CXCR4$^+$ cells (Fig 2D). In contrast, there was a notable decline in the CD34$^-$CD7$^-$CD4$^+$ cell counts in HIV$^+$ samples compared to HIV$^-$ samples at week 3 (Fig 2G). Further analysis of CD34$^-$ cells revealed that the CD7$^+$CD4$^+$ cells contained CD4/CD8 double-positive cells and CD3$^+$CD4$^+$ cells, whereas the CD7$^-$CD4$^+$ cells were mostly CD3$^+$CD4$^+$ cells (Fig S1). In the analysis of CD34$^-$CXCR4$^+$, CD34$^-$CD7$^+$CXCR4$^+$, and CD34$^-$CD7$^-$CXCR4$^+$ cells, the

$CD34^{-}CD7^{-}CXCR4^{+}$ cells were most severely impaired in growth by HIV-1 infection (Figure S2 A-C).

The dynamics of $CD34^{+}$ cells in the OP9-DL1 cocultures with HIV-preexposed $CD34^{+}$ cells

HIV infection of $CD34^{+}$ cells were detected by intracellular $p24^{+}$ staining followed by flow cytometric analysis (Fig 3A-C). Interestingly, there was a steep decline in the average $p24^{+}CD34^{+}$ percentage at week 2 post infection (Fig 3A and B). Also, the $p24^{+}CD34^{+}$ cells failed to grow in number (Fig 3C) in contrast to the rapid growth of $p24^{+}$ cell counts at week 2 (Fig 1F). The $p24^{+}CD34^{+}CD7^{+}$ frequencies didn't show the decline at week 2 (Fig 3D and E). This was due to the low average $CD34^{+}CD7^{+}$ cell count at week 1 and its rapid increase at week 2 post infection (Fig 3H). Accordingly, the $p24^{+}CD34^{+}CD7^{+}$ cell counts increased at weeks 2 and 3 (Fig 3F).

There were nonsignificant differences in $CD34^{+}$ and $CD34^{+}CD7^{+}$ cell counts between HIV^{+} and HIV^{-} cocultures from week 3 until 5. The difference in the average $CD34^{+}$ and $CD34^{+}CD7^{+}$ frequencies were greatest at week 3 (Fig 3G and H). Cells were further evaluated for CXCR4 expression in $CD34^{+}$ cells. Although the data didn't show significant differences between HIV^{+} and HIV^{-} samples, the average $CD34^{+}CXCR4^{+}$, $CD34^{+}CD7^{+}CXCR4^{+}$, and $CD34^{+}CD7^{-}CXCR4^{+}$ cell counts in HIV^{+} cocultures became lower than HIV^{-} cocultures at week 2 (Fig 3I-K). This was earlier than the time point (week 3) at which the average $CD34^{+}$ and $CD34^{+}CD7^{+}$ cell counts in HIV^{+} samples became lower than HIV^{-} samples (Fig 3G and H). Therefore, $CD34^{+}CXCR4^{+}$ cells may be affected by HIV-1 more quickly than the whole $CD34^{+}$ cells.

HIV-1_{NL4-3} infection of HSPC-derived cells after 4-6 weeks' coculture with OP9-DL1

Experiment 1 (Figs 1-4) suggested different cellular dynamics of $CD34^+CD7^+CXCR4^+$ cells than the cells of other phenotypes. To better describe the effect of HIV infection on the short-term dynamics of $CD34^+$ cells, experiment 2 was performed (short coculture, n=12, Fig 4A). The experiment 2 results are shown in Figures 4-6, S4-5, and Tables 1-2. Briefly, the OP9-DL1 coculture with cord-derived $CD34^+$ cells, without HIV infection, produced a mixture of cells with different phenotypes as determined by the expression of CD34, CD4, CD8, CD7, and CXCR4, in 4-6 weeks. Cells were then harvested and infected with HIV-1_{NL4-3}. The infected cells were cocultured again with a new OP9-DL1 monolayer and further incubated for 1 week. Cells were then collected, surface stained, intracellularly stained with anti-HIV-1 p24, and analyzed by flow cytometry. The CD4 expression levels in $CD34^+$ cells before infection were limited and much lower than those in $CD34^-$ cells (Fig 4C). One week after infection, HIV replication was detected in all the HIV-infected samples (Fig 4D). The majority of HIV-1 $p24^+$ cells were $CD34^-$ (Fig 4B). The $p24^+$ cells were partly $CD4^{lo}$, possibly due to CD4 down regulation in HIV infected cells (Fig 4B). The 9 samples tested here showed the average HIV $p24^+$ frequency of 0.31%, the average $p24^+CD34^+$ frequency of 0.03%, and the average $p24^+CD34^+CD7^+$ frequency of 0.02% (Fig 4D). This means that the majority of $p24^+CD34^+$ cells were $CD7^+$ (Fig 4D, Table 1).

Partial loss of $CD34^+CD7^+CXCR4^+$ cells after HIV-1_{NL4-3} infection of OP9-DL1-cocultured cells

The phenotypes of the cells in experiment 2 (short coculture) were analyzed 1 week after infection. The whole cell counts were obtained with part of the batches tested and not significantly different between HIV^+ and HIV^- samples (n=4, p=0.5000, Table

2). The $CD4^+CD8^+$, $CD34^+$, or $CD34^+CD7^+$ frequencies were not significantly different between HIV^+ and HIV^- cocultures (Fig. 5B). When we focused on CXCR4 expression levels in different subsets, the $CD34^+CXCR4^+$, or $CD34^+CD7^-CXCR4^+$ frequencies were not significantly different between HIV^+ and HIV^- cocultures (Fig. 5C left and right). However, the $CD34^+CD7^+CXCR4^+$ frequencies in HIV^+ samples were significantly reduced compared to HIV^- samples (Fig 5A and C middle). This may be in accordance with the results in Fig 3J in which the growth of $CD34^+CD7^+CXCR4^+$ cell counts slowed down earlier (at week 2) than the cell counts of other phenotypes (at week 3).

Increased number of $CD34^+CD7^+CD4^+$ cells after HIV-1_{NL4-3} infection of OP9-DL1-cocultured cells

The Fig 5 results indicated distinct dynamics of $CD34^+CD7^+CXCR4^+$ cells in the presence of HIV-1. To better understand this, $CD34^+CD7^+$ cells were further analyzed for the expression of CD4. Surprisingly, HIV-infected samples had higher $CD34^+CD7^+CD4^+$ frequencies than uninfected samples (Fig 6A and B). These cells were found to be partially HIV $p24^+$ after careful adjustment of compensation matrices of the flow cytometry data (Fig 6A). One out of 9 batches were selected for further analyses of $CD34^+CD7^+CD4^+$ cells. Not only the frequencies but the CD4 fluorescence intensities (FIs) of $CD34^+CD7^+CD4^+$ cells were higher in HIV^+ than in HIV^- samples (Fig 6C). In addition, the CD4 FIs of $CD34^+CD7^+CD4^+$ cells may be inversely correlated with the CD34 FIs (Fig 6D).

The impact of HIV infection on the $CD34^+CD7^+CD4^+$ cells were further analyzed. As shown in Fig 6E, $CD34^+CD7^+CD4^+$ cells in HIV^+ samples had higher p24 mean fluorescence intensities than HIV^- samples, indicating that at least part of those cells

was producing HIV antigens. In addition, the $CD34^{+}CD7^{+}CD4^{+}CXCR4^{+}$ frequencies correlated with the $p24^{+}$ frequencies (Fig 6F).

Discussion

The impact of HIV infection on the bone marrow/thymus functions has been of great interest. The T-cell restoration by antiretroviral drug treatment appears to be critical in control of disease in HIV-infected patients. However, it has been unclear how HIV impacts the T-cell differentiation process. For this purpose, an in vitro model to mimic the process may be helpful. The present study demonstrates the way to utilize the OP9-DL1 coculture system that enables in vitro follow up of the early events in T-cell differentiation such as lymphoid progenitor cell generation, that normally occurs in the bone marrow, and $CD4^+$ thymocyte differentiation in the thymus.

Human HSPC were not considered a major virus reservoir (Durand et al., 2012; von Laer et al., 1990). However, HIV-1 was shown to infect those cells (Carter et al., 2010). Although an article reported negative results on detection of HIV-1 DNA in $CD34^+$ hematopoietic progenitor cells (Josefsson et al., 2012), another study showed that $CD133^+$ hematopoietic stem cells could harbor HIV-1 DNA despite long-term viral control (McNamara et al., 2013). A report says there are preintegration mechanisms to limit HIV infection (Griffin and Goff, 2015). It is still debatable whether HSPCs are an unignorable viral reservoir (Pace and O'Doherty, 2013). There is also a concern for indirect modification of HSPCs and hematopoiesis dynamics through HIV infection and depletion of $CD4^+$ cells. HIV disease is known to accompany bone marrow abnormalities (Tripathi et al., 2005). Some patients fail to show $CD4^+$ T-cell recovery even after effective antiretroviral therapy and are called immunological nonresponders. Such immunological nonresponsiveness can be associated with immune activation and/or bone marrow impairment (Hunt et al., 2003; Isgro et al., 2008).

CXCR4 and its ligand SDF-1 have a variety of roles in biological events such as embryogenesis, angiogenesis, hematopoiesis, and lymphopoiesis. CXCR4 is abundantly expressed in mouse embryos and involved in neuronal, vascular, hematopoietic, cardiac, craniofacial, and gastric development (McGrath et al., 1999). The role of a CXCR4 homologue in zebrafish embryosis has been reported (Raz and Mahabaleshwar, 2009). Development of renal vasculature in mice requires the functions of SDF-1 and CXCR4 (Takabatake et al., 2009). CXCR4 acts as a co-stimulator during thymic β-selection (Trampont et al., 2010).

The events observed in the coculture of OP9-DL1 and human $CD34^+$ cells are likely to involve interaction between SDF-1 and CXCR4, since mouse SDF-1 expressed by OP9-DL1 has high identity of amino acid sequence to human SDF-1 (Shirozu et al., 1995). The observation is in accordance with the previous reports showing that SDF-1/CXCR4 pair is crucially involved in homing and repopulation of HSPCs in the specific BM niches (Moll and Ransohoff, 2010) and also in the whole T-cell developmental process in the thymus (Petrie, 2003; Plotkin et al., 2003).

It has been reported that HSPCs and thymocytes express CXCR4 but their CCR5 expression is limited (Nixon et al., 2013; Taylor et al., 2001). Another report says that HIV utilizes CXCR4 when it infects multipotent progenitor cells (Carter et al., 2011). Although CCR5-tropic HIV-1 strains play an essential role in depletion of CCR5-tropic memory $CD4^+$ T cells leading to AIDS (Schnittman et al., 1990), CXCR4-tropic HIV strains might also contribute to the pathogenesis by interfering with hematopoiesis and/or lymphopoiesis (Akkina, 2013; Bordoni et al., 2015; Ho Tsong Fang et al., 2008). Despite the increasing evidence and interests, it is not yet fully unveiled how CXCR4-tropic HIV-1 strains impair these processes.

The present study results give insights on the impact of HIV-1 persistence upon T-lineage differentiation of hematopoietic progenitor cells. In the first experiment (long coculture), as shown in Figs 1-3 and S1-3, HIV-infected samples showed similar $CD4^+$ cell production rates to uninfected samples at weeks 1 and 2, but reduced $CD4^+$ cell production rates from week 3 until week 5 (Fig 2). This was most clearly observed with the dynamics of $CD34^-CD7^-CD4^+$ cells (Fig 2G) that were mostly $CD3^+$ T cells (Fig S2). It is not clear how the reduction of cell growth at week 3 post infection was so accurately reproduced with all the 12 samples tested (Fig 2G, individual data not shown). However, in the following analyses on $CD34^+$ cells, the growth rates of $CD34^+CD7^+CXCR4^+$ cell counts showed a tendency to drop as early as week 2 (Fig 3J). This was observed with 7 out of 12 samples tested (data not shown), and earlier than the time point (week 3) of $CD4^+$ cell reduction. Because $CD34^+CD7^+$ cells represent lymphoid progenitor cells (Hoebeke et al., 2007), their involvement in defining the production rates of $CD4^+$ cells was speculated.

The second experiment (short coculture, Figs 4-6, S4-5, and Tables 1-2) was carried out to check the effects of HIV-1 upon the short-term dynamics of T-lineage cells including progenitors. This resulted in significant alteration of the $CD34^+CD7^+CXCR4^+$ frequencies 1 week after infection (Fig 5C middle), which may be consistent with the results of the experiment 1 (Fig 3J). Because of the limitation of the present study, the fate of the lost $CD34^+CD7^+CXCR4^+$ cells in the HIV^+ cocultures are unknown. The differentiation capacity of the remaining $CD34^+CD7^+CXCR4^+$ cells also remain untested. Interestingly, a recent article reported that bone marrow $CD34^+$ progenitor cells from HIV-infected patients show an impaired T cell differentiation potential (Bordoni et al., 2017), which was related to proinflammatory cytokines.

Cytokine analyses may be applicable to the coculture assays we established in the present study.

The $CD34^+CD7^+$ lymphoid progenitors were further analyzed to better understand its association with HIV-1 infection. Interestingly, there was an increase in the $CD34^+CD7^+CD4^+$ frequencies in HIV-infected samples compared to uninfected samples (Fig 6). In addition, those $CD34^+CD7^+CD4^+$ cells were found to be partially HIV $p24^+$ (Fig 6A and E). The compensation matrices of the flow cytometry data were checked carefully to exclude false positive results. It may be fascinating to interpret the results as CD4 upregulation following HIV infection, thereby driving the differentiation of T-lineage precursor cells. However, caution may be necessary because the limitation of the study didn't allow exclusion of possible CD34 upregulation in the infected $CD4^+$ cells (Fig S5), although the flow cytometry data didn't indicate correlation between HIV p24 expression and CD34 upregulation in $CD34^{low}$ cells (data not shown). Further studies may be designed to test shorter coculture period than 1 week and/or investigate on the association of HIV-1 infection with factors that regulate the expression of CD3, CD4, CD7, and CD34.

The findings in this article may highlight anti-HIV treatments such as a gene therapy of $CD34^+$ HSPCs followed by transplantation, because in this way the whole hematopoietic events in the host can be placed under protection against HIV infection even in the absence of effective immune response (Savkovic et al., 2014). The problem is that, while CCR5 may be considered a good target for knockout or knockdown to prevent infection of CCR5-tropic HIV strains, the CXCR4 expression levels should not be altered in HSPCs because of the essential biological functions of the molecule (Liu et al., 2014). Therefore, instead of modulation of CXCR4 expression, anti-HIV modalities targeting an HIV gene or component may be desirable for protection of

hematopoietic cells including T-lineage cells from CXCR4-tropic HIV infection (Suzuki et al., 2015; Suzuki et al., 2013).

In summary, the results of the long/short coculture of human $CD34^+$ cells and derivatives with OP9-DL1 in the presence of HIV-1 indicate that the dynamics of $CD34^+CD7^+$ lymphoid progenitors may be affected more quickly by HIV-1 than $CD34^-CD4^+$ thymocytes and T cells despite the lower susceptibility of $CD34^+CD7^+$ cells to HIV-1 infection as suggested by their lower CD4 expression levels. Further studies may be directed against elucidation of the underling mechanisms. In addition, the longer time necessary for the reduction of $CD34^-CD4^+$ cell growth in the HIV^+ cocultures compared to the HIV^- cocultures may implicate the way in which lowered T-cell production rates influence the reduction of $CD4^+$ T-cell counts in HIV-infected patients, in combination with other mechanisms of $CD4^+$ T-cell depletion including the direct cytopathic effect, apoptosis, as well as antigen-specific immunological mechanisms (Costin, 2007; McMichael et al., 2000; Tsukamoto et al., 2016).

Author contributions

Designed the study: TT, SO. Provided cell lines and resources: TT, SO. Performed the experiments: TT. Analyzed the data: TT. Wrote the manuscript: TT. All authors read and approved the final manuscript.

Conflict of interest statement

The authors declare no conflict of interest associated with the present work.

Acknowledgements

We cordially thank Dr. Kazuo Matsui and Dr. Shoichi Kawakami of Fukuda Hospital, Kumamoto, Japan, for their help on cord blood sampling. This work was supported by the National Health and Medical Research Council, Australia (Project grant). It was also partially supported by grants from the following organizations: the Japan Agency for Medical Research and Development (Research program on HIV/AIDS, No. 16fk0410108h0001); Ministry of Education, Culture, Sports, Science and Technology, Japan (Grants-in-Aid for Science Research, No. 25114711); and Kumamoto University (AIDS International Collaborative Research Grant). We specially thank Prof. Anthony D. Kelleher and Dr. Kazuo Suzuki of the Kirby Institute for infection and immunity for society, UNSW Australia, for their support for the whole project, which was planned by UNSW Australia and hosted by Kumamoto University, Japan, from a distance.

References

Adachi, A., Gendelman, H.E., Koenig, S., Folks, T., Willey, R., Rabson, A., Martin, M.A., 1986. Production of acquired immunodeficiency syndrome-associated retrovirus in human and nonhuman cells transfected with an infectious molecular clone. Journal of virology 59, 284-291.

Akkina, R., 2013. New insights into HIV impact on hematopoiesis. Blood 122, 2144-2146.

Alexaki, A., Wigdahl, B., 2008. HIV-1 infection of bone marrow hematopoietic progenitor cells and their role in trafficking and viral dissemination. PLoS pathogens 4, e1000215.

Banda, N.K., Simon, G.R., Sipple, J.D., Terrell, K.L., Archer, P., Shpall, E.J., Akkina, R.K., Myers, A.M., Harrison, G.S., 1999. Depletion of CD34+ CD4+ cells in bone marrow from HIV-1-infected individuals. Biology of blood and marrow transplantation : journal of the American Society for Blood and Marrow Transplantation 5, 162-172.

Blom, M., Epeldegui, M., Uittenbogaart, C.H., 2011. Factors Contributing to HIV-1 Induced Pathogenesis in the Human Thymus, in: Chang, T.L.-Y. (Ed.), HIV-Host Interactions. InTech.

Bordoni, V., Bibas, M., Viola, D., Sacchi, A., Cimini, E., Tumino, N., Casetti, R., Amendola, A., Ammassari, A., Agrati, C., Martini, F., 2017. Bone Marrow CD34+ Progenitor Cells from HIV-Infected Patients Show an Impaired T Cell Differentiation Potential Related to Proinflammatory Cytokines. AIDS research and human retroviruses 33, 590-596.

Bordoni, V., Casetti, R., Viola, D., Abbate, I., Rozera, G., Sacchi, A., Cimini, E., Tumino, N., Agrati, C., Orchi, N., Pinnetti, C., Ammassari, A., Martini, F., 2015. Early ART in primary HIV infection may also preserve lymphopoiesis capability in circulating haematopoietic progenitor cells: a case report. The Journal of antimicrobial chemotherapy.

Carter, C.C., McNamara, L.A., Onafuwa-Nuga, A., Shackleton, M., Riddell, J.t., Bixby, D., Savona, M.R., Morrison, S.J., Collins, K.L., 2011. HIV-1 utilizes the CXCR4 chemokine receptor to infect multipotent hematopoietic stem and progenitor cells. Cell host & microbe 9, 223-234.

Carter, C.C., Onafuwa-Nuga, A., McNamara, L.A., Riddell, J.t., Bixby, D., Savona, M.R., Collins, K.L., 2010. HIV-1 infects multipotent progenitor cells causing cell death and establishing latent cellular reservoirs. Nature medicine 16, 446-451.

Corbeau, P., Reynes, J., 2011. Immune reconstitution under antiretroviral therapy: the new challenge in HIV-1 infection. Blood 117, 5582-5590.

Costin, J.M., 2007. Cytopathic mechanisms of HIV-1. Virol J 4, 100.

De Smedt, M., Hoebeke, I., Plum, J., 2004. Human bone marrow CD34+ progenitor cells mature to T cells on OP9-DL1 stromal cell line without thymus microenvironment. Blood cells, molecules & diseases 33, 227-232.

Dudek, T.E., Allen, T.M., 2013. HIV-specific CD8(+) T-cell immunity in humanized bone marrow-liver-thymus mice. The Journal of infectious diseases 208 Suppl 2, S150-154.

Durand, C.M., Ghiaur, G., Siliciano, J.D., Rabi, S.A., Eisele, E.E., Salgado, M., Shan, L., Lai, J.F., Zhang, H., Margolick, J., Jones, R.J., Gallant, J.E., Ambinder, R.F., Siliciano, R.F., 2012. HIV-1 DNA is detected in bone marrow populations containing CD4+ T cells but is not found in purified CD34+ hematopoietic progenitor

cells in most patients on antiretroviral therapy. The Journal of infectious diseases 205, 1014-1018.

Griffin, D.O., Goff, S.P., 2015. HIV-1 Is Restricted prior to Integration of Viral DNA in Primary Cord-Derived Human CD34+ Cells. Journal of virology 89, 8096-8100.

Grivel, J.C., Margolis, L.B., 1999. CCR5- and CXCR4-tropic HIV-1 are equally cytopathic for their T-cell targets in human lymphoid tissue. Nature medicine 5, 344-346.

Ho Tsong Fang, R., Colantonio, A.D., Uittenbogaart, C.H., 2008. The role of the thymus in HIV infection: a 10 year perspective. AIDS (London, England) 22, 171-184.

Hoebeke, I., De Smedt, M., Stolz, F., Pike-Overzet, K., Staal, F.J., Plum, J., Leclercq, G., 2007. T-, B- and NK-lymphoid, but not myeloid cells arise from human CD34(+)CD38(-)CD7(+) common lymphoid progenitors expressing lymphoid-specific genes. Leukemia 21, 311-319.

Holmes, R., Zuniga-Pflucker, J.C., 2009. The OP9-DL1 system: generation of T-lymphocytes from embryonic or hematopoietic stem cells in vitro. Cold Spring Harbor protocols 2009, pdb.prot5156.

Hunt, P.W., Martin, J.N., Sinclair, E., Bredt, B., Hagos, E., Lampiris, H., Deeks, S.G., 2003. T cell activation is associated with lower CD4+ T cell gains in human immunodeficiency virus-infected patients with sustained viral suppression during antiretroviral therapy. The Journal of infectious diseases 187, 1534-1543.

Isgro, A., Leti, W., De Santis, W., Marziali, M., Esposito, A., Fimiani, C., Luzi, G., Pinti, M., Cossarizza, A., Aiuti, F., Mezzaroma, I., 2008. Altered clonogenic capability and stromal cell function characterize bone marrow of HIV-infected

subjects with low CD4+ T cell counts despite viral suppression during HAART. Clin Infect Dis 46, 1902-1910.

Janas, M.L., Varano, G., Gudmundsson, K., Noda, M., Nagasawa, T., Turner, M., 2010. Thymic development beyond beta-selection requires phosphatidylinositol 3-kinase activation by CXCR4. The Journal of experimental medicine 207, 247-261.

Josefsson, L., Eriksson, S., Sinclair, E., Ho, T., Killian, M., Epling, L., Shao, W., Lewis, B., Bacchetti, P., Loeb, L., Custer, J., Poole, L., Hecht, F.M., Palmer, S., 2012. Hematopoietic precursor cells isolated from patients on long-term suppressive HIV therapy did not contain HIV-1 DNA. The Journal of infectious diseases 206, 28-34.

Knutsen, A.P., Roodman, S.T., Freeman, J.J., Mueller, K.R., Bouhasin, J.D., 1999. Inhibition of thymopoiesis of CD34+ cell maturation by HIV-1 in an in vitro CD34+ cell and thymic epithelial organ culture model. Stem cells (Dayton, Ohio) 17, 327-338.

Kucia, M., Jankowski, K., Reca, R., Wysoczynski, M., Bandura, L., Allendorf, D.J., Zhang, J., Ratajczak, J., Ratajczak, M.Z., 2004. CXCR4-SDF-1 signalling, locomotion, chemotaxis and adhesion. Journal of molecular histology 35, 233-245.

Kucia, M., Reca, R., Miekus, K., Wanzeck, J., Wojakowski, W., Janowska-Wieczorek, A., Ratajczak, J., Ratajczak, M.Z., 2005. Trafficking of normal stem cells and metastasis of cancer stem cells involve similar mechanisms: pivotal role of the SDF-1-CXCR4 axis. Stem cells (Dayton, Ohio) 23, 879-894.

Lapidot, T., Kollet, O., 2002. The essential roles of the chemokine SDF-1 and its receptor CXCR4 in human stem cell homing and repopulation of transplanted immune-deficient NOD/SCID and NOD/SCID/B2m(null) mice. Leukemia 16, 1992-2003.

Liu, Y., Zhou, J., Pan, J.A., Mabiala, P., Guo, D., 2014. A novel approach to block HIV-1 coreceptor CXCR4 in non-toxic manner. Molecular biotechnology 56, 890-902.

Marsden, M.D., Kovochich, M., Suree, N., Shimizu, S., Mehta, R., Cortado, R., Bristol, G., An, D.S., Zack, J.A., 2012. HIV latency in the humanized BLT mouse. Journal of virology 86, 339-347.

McGrath, K.E., Koniski, A.D., Maltby, K.M., McGann, J.K., Palis, J., 1999. Embryonic expression and function of the chemokine SDF-1 and its receptor, CXCR4. Developmental biology 213, 442-456.

McMichael, A.J., Ogg, G., Wilson, J., Callan, M., Hambleton, S., Appay, V., Kelleher, T., Rowland-Jones, S., 2000. Memory CD8+ T cells in HIV infection. Philosophical transactions of the Royal Society of London. Series B, Biological sciences 355, 363-367.

McNamara, L.A., Onafuwa-Nuga, A., Sebastian, N.T., Riddell, J.t., Bixby, D., Collins, K.L., 2013. CD133+ hematopoietic progenitor cells harbor HIV genomes in a subset of optimally treated people with long-term viral suppression. The Journal of infectious diseases 207, 1807-1816.

Mohtashami, M., Shah, D.K., Nakase, H., Kianizad, K., Petrie, H.T., Zuniga-Pflucker, J.C., 2010. Direct comparison of Dll1- and Dll4-mediated Notch activation levels shows differential lymphomyeloid lineage commitment outcomes. Journal of immunology (Baltimore, Md. : 1950) 185, 867-876.

Moll, N.M., Ransohoff, R.M., 2010. CXCL12 and CXCR4 in bone marrow physiology. Expert review of hematology 3, 315-322.

Nakano, T., Kodama, H., Honjo, T., 1994. Generation of lymphohematopoietic cells from embryonic stem cells in culture. Science (New York, N.Y.) 265, 1098-1101.

Nixon, C.C., Vatakis, D.N., Reichelderfer, S.N., Dixit, D., Kim, S.G., Uittenbogaart, C.H., Zack, J.A., 2013. HIV-1 infection of hematopoietic progenitor cells in vivo in humanized mice. Blood 122, 2195-2204.

Okoye, A.A., Picker, L.J., 2013. CD4(+) T-cell depletion in HIV infection: mechanisms of immunological failure. Immunological reviews 254, 54-64.

Pace, M., O'Doherty, U., 2013. Hematopoietic stem cells and HIV infection. The Journal of infectious diseases 207, 1790-1792.

Parinitha, S.S., Kulkarni, M.H., 2012. Haematological changes in HIV infection with correlation to CD4 cell count. The Australasian Medical Journal 5, 157-162.

Petrie, H.T., 2003. Cell migration and the control of post-natal T-cell lymphopoiesis in the thymus. Nature reviews. Immunology 3, 859-866.

Plotkin, J., Prockop, S.E., Lepique, A., Petrie, H.T., 2003. Critical role for CXCR4 signaling in progenitor localization and T cell differentiation in the postnatal thymus. Journal of immunology (Baltimore, Md. : 1950) 171, 4521-4527.

Raz, E., Mahabaleshwar, H., 2009. Chemokine signaling in embryonic cell migration: a fisheye view. Development (Cambridge, England) 136, 1223-1229.

Savkovic, B., Nichols, J., Birkett, D., Applegate, T., Ledger, S., Symonds, G., Murray, J.M., 2014. A quantitative comparison of anti-HIV gene therapy delivered to hematopoietic stem cells versus CD4+ T cells. PLoS computational biology 10, e1003681.

Schmitt, T.M., de Pooter, R.F., Gronski, M.A., Cho, S.K., Ohashi, P.S., Zuniga-Pflucker, J.C., 2004. Induction of T cell development and establishment of T cell competence from embryonic stem cells differentiated in vitro. Nature immunology 5, 410-417.

Schnittman, S.M., Lane, H.C., Greenhouse, J., Justement, J.S., Baseler, M., Fauci, A.S., 1990. Preferential infection of CD4+ memory T cells by human immunodeficiency virus type 1: evidence for a role in the selective T-cell functional defects observed in infected individuals. Proceedings of the National Academy of Sciences of the United States of America 87, 6058-6062.

Shirozu, M., Nakano, T., Inazawa, J., Tashiro, K., Tada, H., Shinohara, T., Honjo, T., 1995. Structure and chromosomal localization of the human stromal cell-derived factor 1 (SDF1) gene. Genomics 28, 495-500.

Suzuki, H., Motohara, M., Miyake, A., Ibuki, K., Fukazawa, Y., Inaba, K., Masuda, K., Minato, N., Kawamoto, H., Hayami, M., Miura, T., 2005a. Intrathymic effect of acute pathogenic SHIV infection on T-lineage cells in newborn macaques. Microbiology and immunology 49, 667-679.

Suzuki, K., Ahlenstiel, C., Marks, K., Kelleher, A.D., 2015. Promoter Targeting RNAs: Unexpected Contributors to the Control of HIV-1 Transcription. Molecular therapy. Nucleic acids 4, e222.

Suzuki, K., Hattori, S., Marks, K., Ahlenstiel, C., Maeda, Y., Ishida, T., Millington, M., Boyd, M., Symonds, G., Cooper, D.A., Okada, S., Kelleher, A.D., 2013. Promoter Targeting shRNA Suppresses HIV-1 Infection In vivo Through Transcriptional Gene Silencing. Molecular therapy. Nucleic acids 2, e137.

Suzuki, K., Shijuuku, T., Fukamachi, T., Zaunders, J., Guillemin, G., Cooper, D., Kelleher, A., 2005b. Prolonged transcriptional silencing and CpG methylation

induced by siRNAs targeted to the HIV-1 promoter region. J RNAi Gene Silencing 1, 66-78.

Takabatake, Y., Sugiyama, T., Kohara, H., Matsusaka, T., Kurihara, H., Koni, P.A., Nagasawa, Y., Hamano, T., Matsui, I., Kawada, N., Imai, E., Nagasawa, T., Rakugi, H., Isaka, Y., 2009. The CXCL12 (SDF-1)/CXCR4 axis is essential for the development of renal vasculature. Journal of the American Society of Nephrology : JASN 20, 1714-1723.

Taylor, J.R., Jr., Kimbrell, K.C., Scoggins, R., Delaney, M., Wu, L., Camerini, D., 2001. Expression and function of chemokine receptors on human thymocytes: implications for infection by human immunodeficiency virus type 1. Journal of virology 75, 8752-8760.

Trampont, P.C., Tosello-Trampont, A.C., Shen, Y., Duley, A.K., Sutherland, A.E., Bender, T.P., Littman, D.R., Ravichandran, K.S., 2010. CXCR4 acts as a costimulator during thymic beta-selection. Nature immunology 11, 162-170.

Tripathi, A.K., Misra, R., Kalra, P., Gupta, N., Ahmad, R., 2005. Bone marrow abnormalities in HIV disease. The Journal of the Association of Physicians of India 53, 705-710.

Tsukamoto, T., Okada, S., 2017. The use of RetroNectin in studies requiring in vitro HIV-1 infection of human hematopoietic stem/progenitor cells. Journal of virological methods 248, 234-237.

Tsukamoto, T., Yamamoto, H., Okada, S., Matano, T., 2016. Recursion-based depletion of human immunodeficiency virus-specific naive CD4(+) T cells may facilitate persistent viral replication and chronic viraemia leading to acquired immunodeficiency syndrome. Medical hypotheses 94, 81-85.

von Laer, D., Hufert, F.T., Fenner, T.E., Schwander, S., Dietrich, M., Schmitz, H., Kern, P., 1990. CD34+ hematopoietic progenitor cells are not a major reservoir of the human immunodeficiency virus. Blood 76, 1281-1286.

Weiss, R.A., 1996. HIV receptors and the pathogenesis of AIDS. Science (New York, N.Y.) 272, 1885-1886.

Ye, P., Kirschner, D.E., Kourtis, A.P., 2004. The thymus during HIV disease: role in pathogenesis and in immune recovery. Current HIV research 2, 177-183.

Figure legends

Figure 1. Primary umbilical cord-derived $CD34^+$ cells are partially susceptible to HIV infection. Coculture of HIV-infected primary cord-derived $CD34^+$ cells with OP9-DL1 resulted in persistent viral replication for five weeks (n=12). (A) Schematic representation of the first experiment (long coculture). Cord-derived $CD34^+$ cells were infected with HIV-1_{NL4-3} and cocultured with OP9-DL1 for 5 weeks. (B) $CD34^+$ cells were gated and tested for expression of CD4 and CXCR4 by flow cytometry. Representative plots are shown. The CD4 signal levels were higher than those of the cells stained with a PE-conjugated mouse isotype control antibody. (C) Intracellular HIV p24 expression was tested 1 week after infection. HIV $p24^+$ cells were found in both $CD34^+$ and $CD34^-$ fractions of HIV-infected samples. Representative plots are shown. (D) $CD34^+$ and $CD34^-$ fractions of an HIV-infected sample were separated by the CD34 microbead method. Total DNA was isolated and analyzed by PCR. HIV *gag* DNA was detected in both $CD34^+$ and $CD34^-$ fractions. A PCR sample using an HIV molecular plasmid pNL4-3 was placed as a control. (E) HIV $p24^+$ percentages in HIV^+ OP9-DL1 coculture samples tested every week by intracellular staining and flow cytometry. (F) HIV $p24^+$ cell counts were calculated from HIV $p24^+$ percentages and whole cell counts. (G) Coculture supernatants of HIV-infected samples were tested for HIV p24 concentrations by using an ELISA at weeks 2-5. (H) Correlation analysis between HIV $p24^+$ frequencies and HIV p24 concentrations. The week 2-5 data in F and G are included (n=48). Spearman's correlation coefficiency is shown.

Figure 2. Preexposure of primary cord-derived $CD34^+$ cells to HIV-1 affected the dynamics of OP9-DL1 cocultured cells (n=12). (A) Whole cell counts were compared

between HIV$^+$ and HIV$^-$ cocultures. (B) Representative plots for those samples that showed reduced CD4$^+$CD8$^+$ frequencies 3-5 weeks after HIV preexposure of primary CD34$^+$ cells and coculture. The plots were selected from week 4 samples. (C-D) Cell counts were compared between HIV$^+$ and HIV$^-$ cocultures for (C) CD4$^+$CD8$^+$ cells, and (D) CD4$^+$CD8$^+$CXCR4$^+$ cell counts were compared between HIV$^+$ and HIV$^-$ cocultures. (E) Representative plots showing the loss of CD34$^-$CD7$^-$CD4$^+$ cells in the HIV-infected cocultures. (F-G) Cell counts were compared between HIV$^+$ and HIV$^-$ cocultures for (F) CD34$^-$CD7$^+$CD4$^+$ cells, and (G) CD34$^-$CD7$^-$CD4$^+$ cells. Statistical analyses were performed by the Wilcoxon matched-pairs signed rank test. **: $p < 0.01$, ***: $p < 0.001$.

Figure 3. Preexposure of primary cord-derived CD34$^+$ cells to HIV-1 affected the dynamics of CD34$^+$ cells in the following OP9-DL1 cocultures (n=12). (A) HIV p24$^+$CD34$^+$ percentages in HIV$^+$ OP9-DL1 coculture samples. (B) The data in Fig 3A were converted to HIV p24$^+$ percentages of CD34$^+$ cells. (C) HIV p24$^+$CD34$^+$ cell counts in HIV$^+$ OP9-DL1 coculture samples. (D) HIV p24$^+$CD34$^+$CD7$^+$ percentages in HIV$^+$ OP9-DL1 coculture samples. (E) The data in Fig 3A were converted to HIV p24$^+$ percentages of CD34$^+$CD7$^+$ cells. (F) HIV p24$^+$CD34$^+$CD7$^+$ cell counts in HIV$^+$ OP9-DL1 coculture samples. (G-K) Cell counts were compared between HIV$^+$ and HIV$^-$ cocultures for (G) CD34$^+$ cells, (H) CD34$^+$CD7$^+$ cells, (I) CD34$^+$CXCR4$^+$ cells, (J) CD34$^+$CD7$^+$CXCR4$^+$ cells, and (K) CD34$^+$CD7$^-$CXCR4$^+$ (right) cell counts. Statistical analyses were performed by the Wilcoxon matched-pairs signed rank test. *: $p < 0.05$.

Figure 4. The experiment 2 (short coculture) was performed to further analyze the dynamics of CD34$^+$ cell in the presence of HIV-1. (A) Schematic representation of the

experiment 2 (short coculture). Primary cord-derived $CD34^+$ cells were cocultured with OP9-DL1 for 4-6 weeks. Cells were then collected and infected with HIV-1_{NL4-3}. The infected cells were cocultured again with OP9-DL1 for 1 week, collected and analyzed. (B) $CD4^+$ percentages in $CD34^-$, $CD34^-CD7^+$, $CD34^-CD7^-$, $CD34^+$, and $CD34^+CD7^+$ subsets before infection. A multiple comparison test was performed to compare $CD34^-$ and $CD34^+$ cells, or $CD34^-CD7^+$ and $CD34^-CD7^-$ cells. (C) Representative plots showing HIV $p24^+$ cells after the post-infection coculture and their phenotypes. The majority of $p24^+$ cells were $CD8^+$ and $CD34^-$. (D) HIV $p24^+$, $p24^+CD34^-CD7^+$, $p24^+CD34^-CD7^-$, $p24^+CD34^+$, and $p24^+CD34^+CD7^+$ frequencies measured 1 week after the post-infection coculture (n=9). Statistical analyses were performed by the Wilcoxon matched-pairs signed rank test, except for the multiple comparison test with the Dunn's method.

Figure 5. $CD34^+$ cells in the experiment 2 (short coculture, as described in Fig 4A) were analyzed after the second (1 week) coculture (n=9). (A) Representative plots showing the CD7/CXCR4 expression levels in $CD34^+$ cells. An HIV^+ sample is compared to its autologous uninfected counterpart. (B) $CD34^+CXCR4^+$ (left), $CD34^+CD7^+CXCR4^+$ (middle left), $CD34^+CD7^+CD4^+CXCR4^+$ (middle right), and $CD34^+CD7^-CXCR4^+$ (right) frequencies were compared between HIV^+ and HIV^- samples. (C) $CD4^+CD8^+CXCR4^+$ (left), $CD34^-CXCR4^+$ (middle left), $CD34^-CD7^+CXCR4^+$ (middle right), and $CD34^-CD7^-CXCR4^+$ (right) frequencies were compared between HIV^+ and HIV^- samples. Statistical analyses were performed by the Wilcoxon matched-pairs signed rank test.

Figure 6. $CD34^+CD7^+$ cells in the experiment 2 (short coculture, as described in Fig 4A) were analyzed after the second (1 week) coculture (n=9 unless otherwise noted). For these analyses, compensation matrices were checked repeatedly to exclude false positive events. (A) Representative plots showing the CD4/CXCR4 and CD4/p24 expression levels in $CD34^+CD7^+$ cells. An HIV^+ sample is compared to its autologous uninfected counterpart. (B) Comparison of $CD34^+CD4^+$ (left), $CD34^+CD7^+CD4^+$ (middle), and $CD34^+CD7^+CD4^+CXCR4^+$ (right) frequencies between HIV^+ and HIV^- samples. (C-D) $CD34^+CD7^+CD4^+$ cells in sample ID 1 (presented in A) were further analyzed. (C) Fluorescence intensities (FIs) of $CD34^+CD7^+CD4^+$ cells were compared between HIV^+ and HIV^- samples by the Mann-Whitney test. (D) Correlation between CD4 FI and CD34 FI of $CD34^+CD7^+CD4^+$ cells in the HIV^+ sample of ID 1 were analyzed (n=3 for HIV^-; n=7 for HIV^+). (E) p24 mean fluorescence intensities (MFIs) of $CD34^+CD7^+CD4^+$ cells were compared between HIV^+ and HIV^- samples (n=7). (F) $CD34^+CD7^+CD4^+CXCR4^+$ cells were tested for correlation with $p24^+$ (left), $p24^+CD34^+$ (middle), and $p24^+CD34^+CD7^+$ (right) frequencies. Comparisons were done by the Wilcoxon matched-pairs signed rank test unless otherwise noted. Spearman's correlation coefficiencies were calculated for correlation analyses.

Tables

Subset	Cell count in infected samples (mean±SD, n=4)	% in the mean whole cell count
Whole	390,000±154,919	100
$p24^+$	547±258	0.140
$p24^+CD34^-CD7^+$	326±242	0.084
$p24^+CD34^-CD7^-$	124±56	0.032
$p24^+CD34^+$	97±42	0.025
$p24^+CD34^+CD7^+$	80±31	0.021

Table 1. Mean cell counts (n=4) in different HIV $p24^+$ subsets of OP9-DL1 cocultured cells. The whole cell count data were obtained with 4 out of the 9 samples of experiment 2 (short coculture, Figs 4-6 and S4-5), in which cord-derived $CD34^+$ cells were first cocultured with OP9-DL1 for 4-6 weeks, infected with HIV-1_{NL4-3}, cocultured again for 1 week, and analyzed by flow cytometry. The percentages in the mean whole cell count are also shown. SD: standard deviation.

Subset	Cell count (mean±SD, n=4)		$\% \frac{(infected-uninfected)}{uninfected}$
	uninfected	*infected*	
Whole	400,000±168,721	390,000±154,919	−2.5
$CD4^+CD8^+$	5,789±3,514	4,919±2,364	**−15.0**
$CD4^+CD8^+CXCR4^+$	3,287±1,757	3,047±1,842	−7.3
$CD34^+$	32,848±18,150	32,107±21,361	−2.3
$CD34^+CD7^+$	16,715±9,521	16,106±12,126	−3.6
$CD34^+CXCR4^+$	18,302±10,987	18,288±14,726	−0.1
$CD34^+CD7^+CXCR4^+$	12,135±7,813	11,892±11,141	−2.0
$CD34^+CD7^-CXCR4^+$	6,151±3,867	6,379±3,989	+3.7
$CD34^+CD7^+CD4^+$	129±42	178±74	**+38.0**
$CD34^-CXCR4^+$	148,493±163,552	157,078±166,602	+5.8
$CD34^-CD7^+CXCR4^+$	131,461±161,042	138,810±162,033	+5.6
$CD34^-CD7^-CXCR4^+$	16,936±7,454	18,261±8,041	+7.8

Table 2. Mean cell counts (n=4) in different subsets of OP9-DL1 cocultured cells. The whole cell count data were obtained with 4 out of the 9 samples of experiment 2 (short coculture, Figs 4-6 and S4-5), in which cord-derived $CD34^+$ cells were first cocultured with OP9-DL1 for 4-6 weeks, infected with HIV-1_{NL4-3}, cocultured again for 1 week, and analyzed by flow cytometry. Cell counts in HIV-infected samples were compared with uninfected control samples. Percent changes of the subset cell counts by HIV infection were calculated and shown in the last column. Percent changes > 10% or < −10% are shown in bold. SD: standard deviation.

Figure 1

A

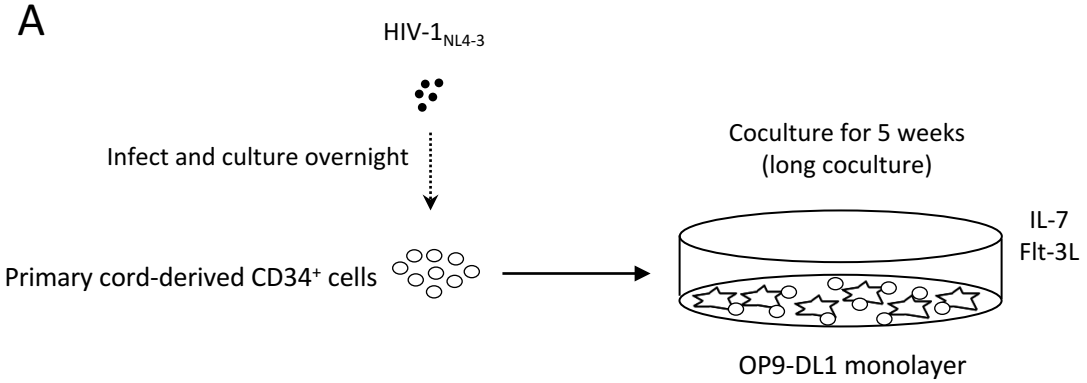

B

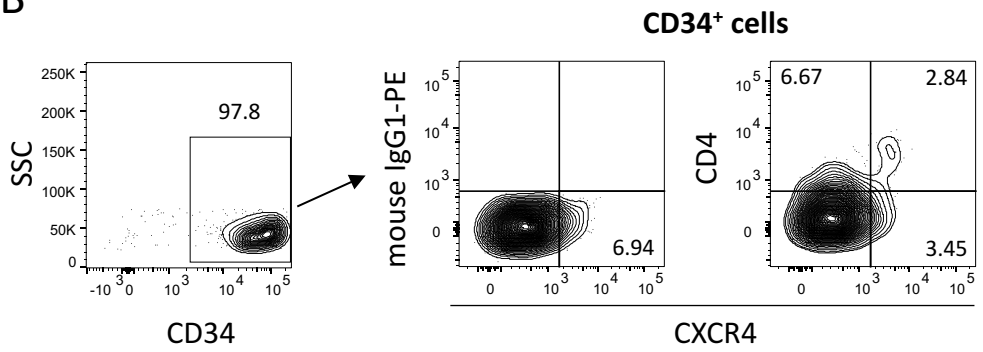

C

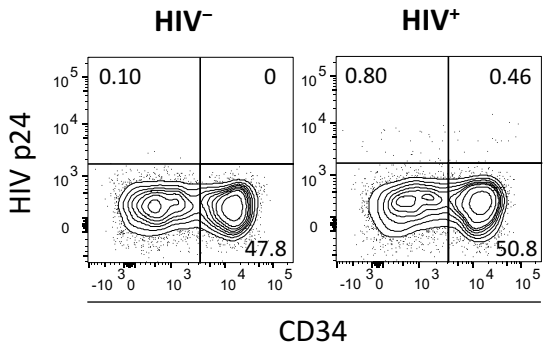

D

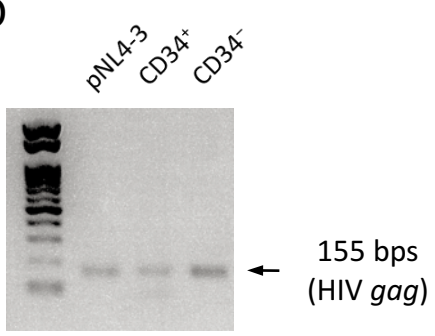

E

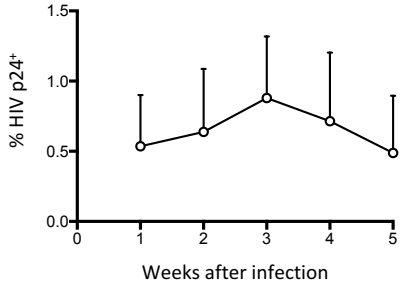

F

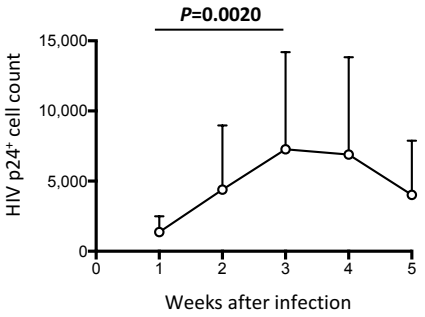

G

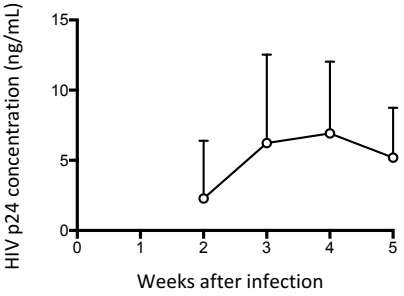

H

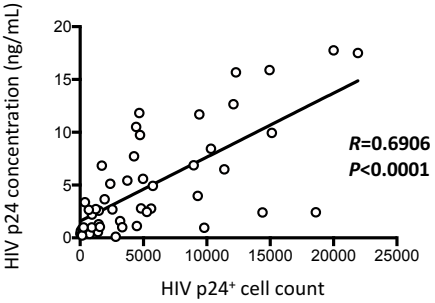

Figure 2

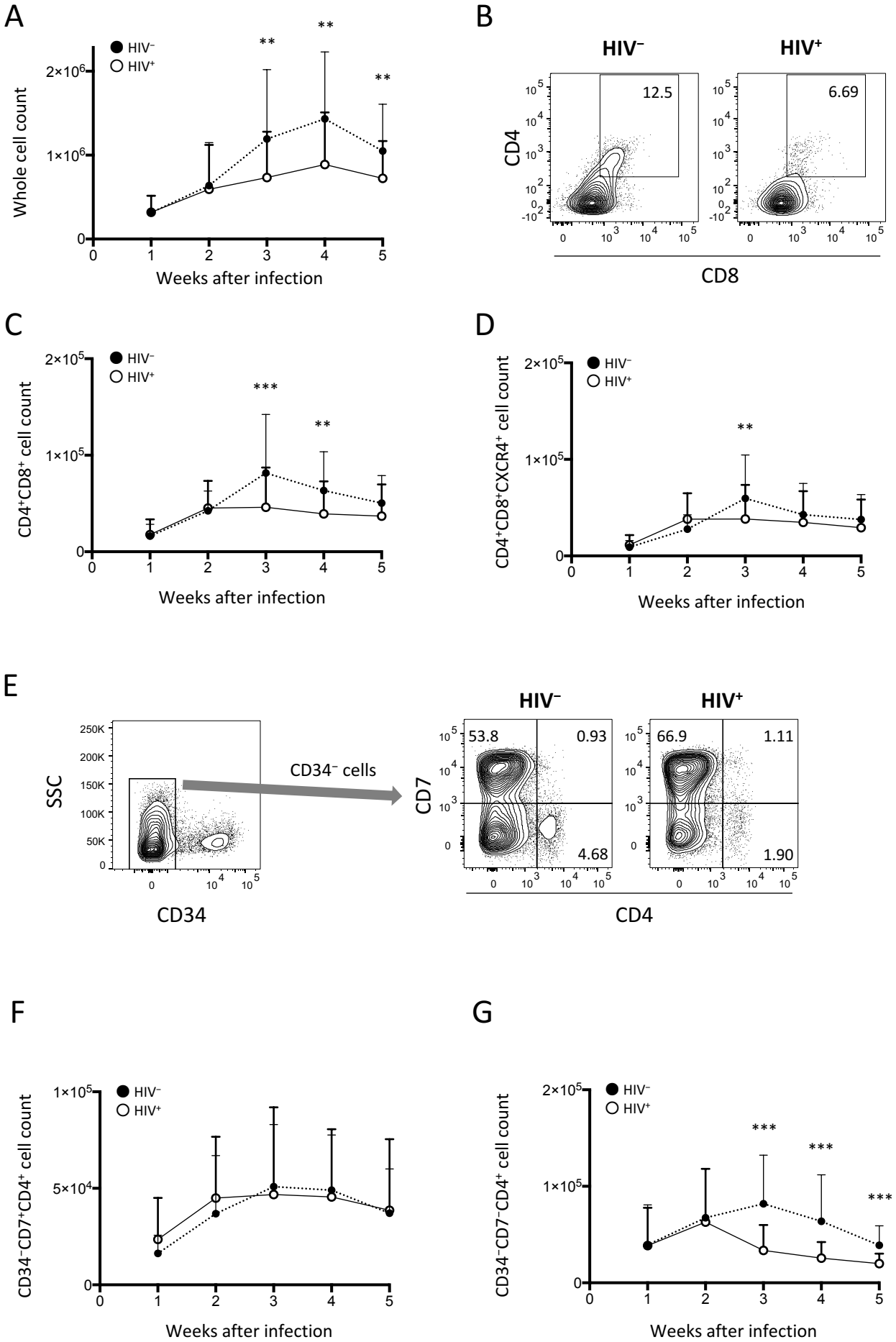
A
HIV⁻
HIV⁺
Whole cell count
Weeks after infection
B
HIV⁻
HIV⁺
12.5
6.69
CD4
CD8
C
CD4⁺CD8⁺ cell count
Weeks after infection
D
CD4⁺CD8⁺CXCR4⁺ cell count
Weeks after infection
E
SSC
CD34
CD34⁻ cells
CD7
CD4
53.8
0.93
4.68
66.9
1.11
1.90
F
CD34⁻CD7⁺CD4⁺ cell count
Weeks after infection
G
CD34⁻CD7⁻CD4⁺ cell count
Weeks after infection

Figure 3

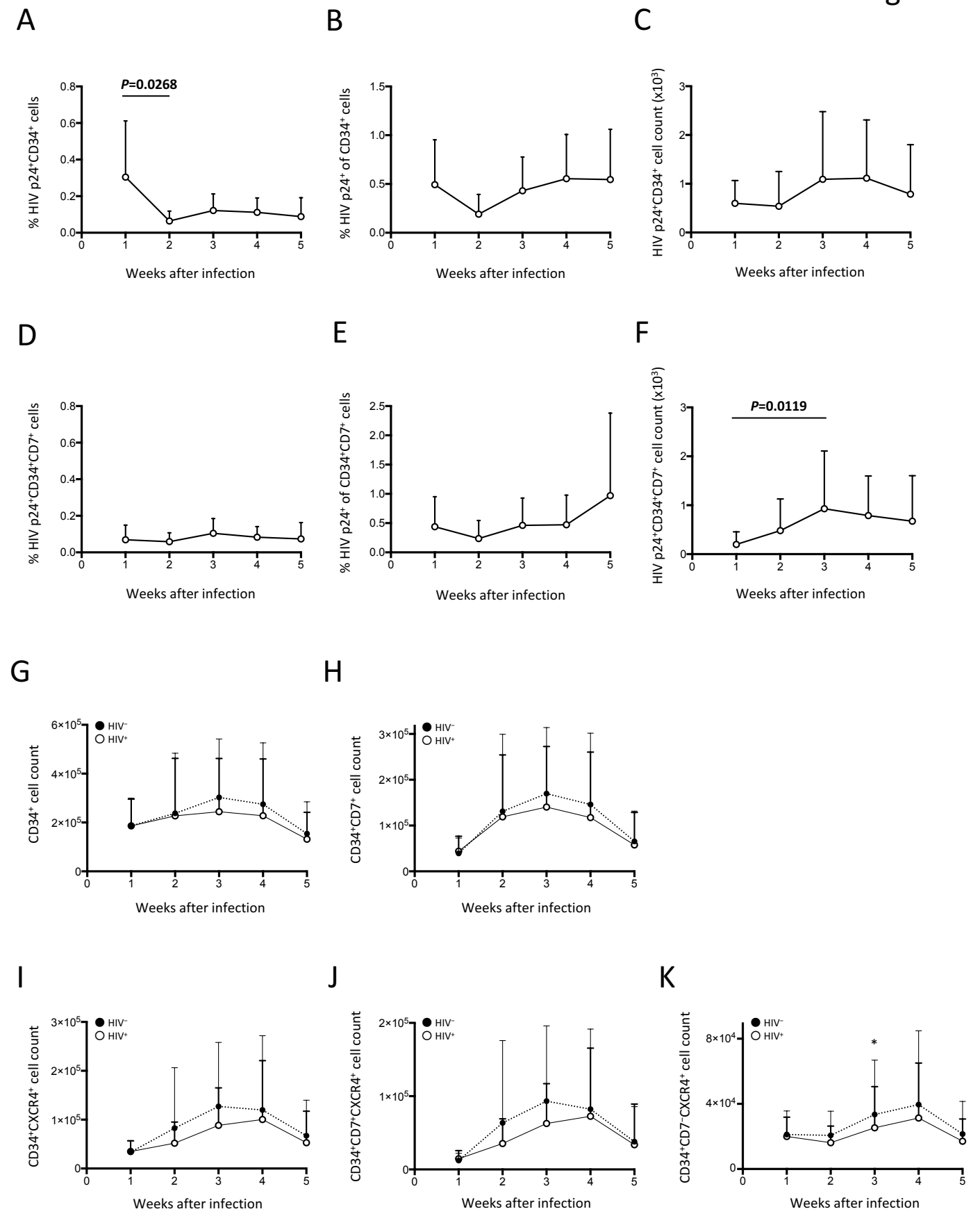
A
P=0.0268
% HIV p24+CD34+ cells
Weeks after infection
B
% HIV p24+ of CD34+ cells
Weeks after infection
C
HIV p24+CD34+ cell count (x10³)
Weeks after infection
D
% HIV p24+CD34+CD7+ cells
Weeks after infection
E
% HIV p24+ of CD34+CD7+ cells
Weeks after infection
F
P=0.0119
HIV p24+CD34+CD7+ cell count (x10³)
Weeks after infection
G
HIV⁻
HIV⁺
CD34+ cell count
Weeks after infection
H
HIV⁻
HIV⁺
CD34+CD7+ cell count
Weeks after infection
I
HIV⁻
HIV⁺
CD34+CXCR4+ cell count
Weeks after infection
J
HIV⁻
HIV⁺
CD34+CD7+CXCR4+ cell count
Weeks after infection
K
HIV⁻
HIV⁺
*
CD34+CD7-CXCR4+ cell count
Weeks after infection

Figure 4

A

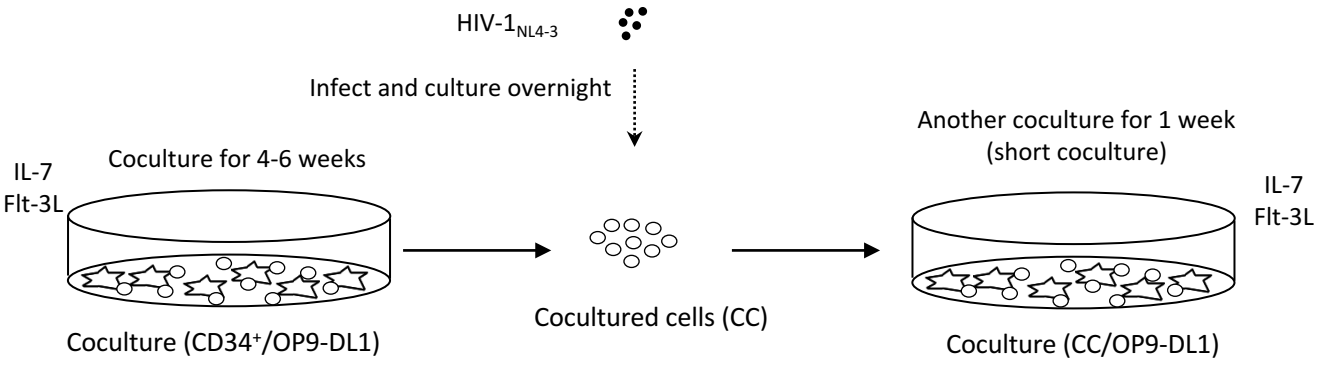

B

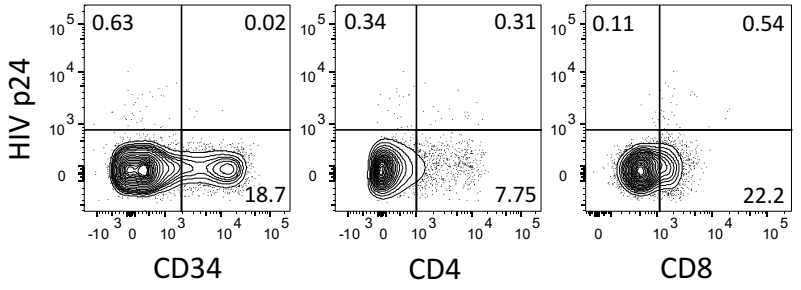

C

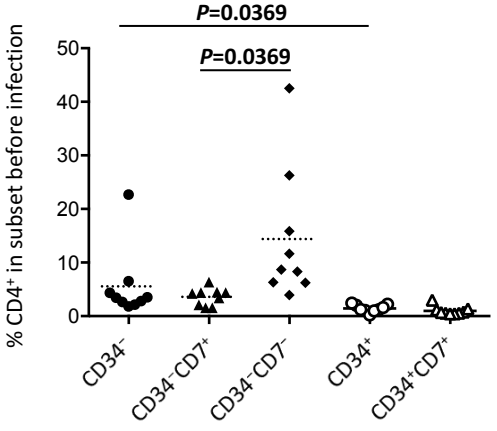

D

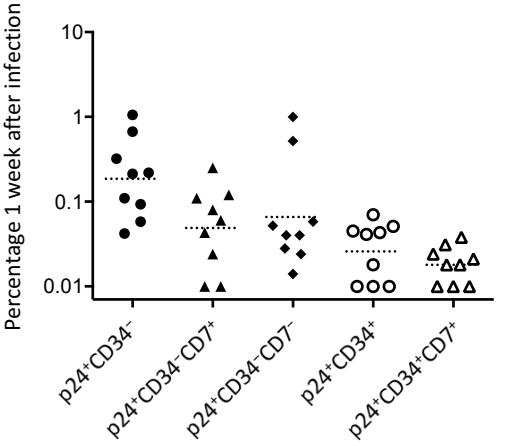

Figure 5

A

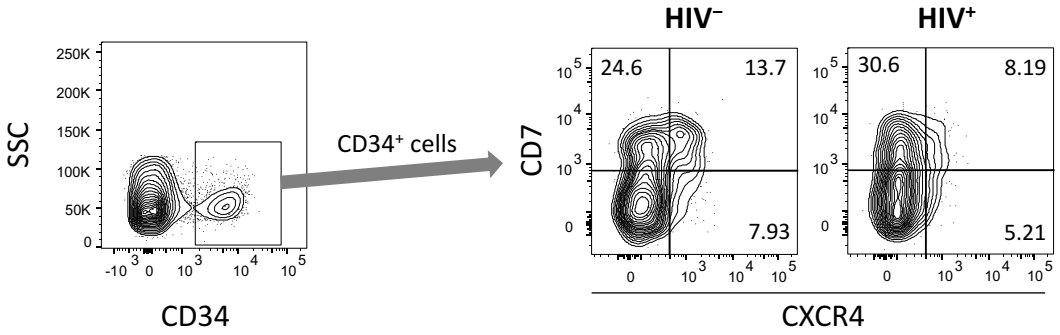
SSC
CD34
CD34+ cells
HIV−
HIV+
CD7
CXCR4
24.6
13.7
7.93
30.6
8.19
5.21

B

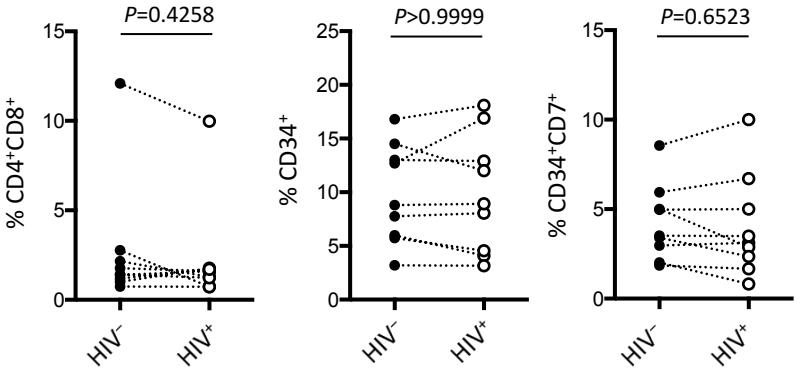
P=0.4258
P>0.9999
P=0.6523
% CD4+CD8+
% CD34+
% CD34+CD7+
HIV−
HIV+

C

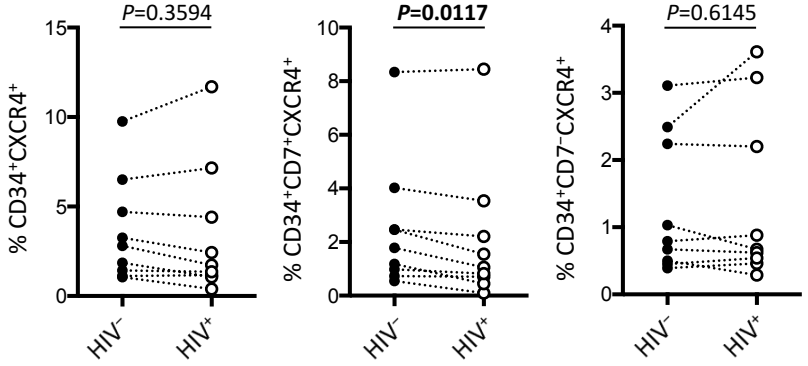
P=0.3594
P=0.0117
P=0.6145
% CD34+CXCR4+
% CD34+CD7+CXCR4+
% CD34+CD7−CXCR4+
HIV−
HIV+

Figure 6

A

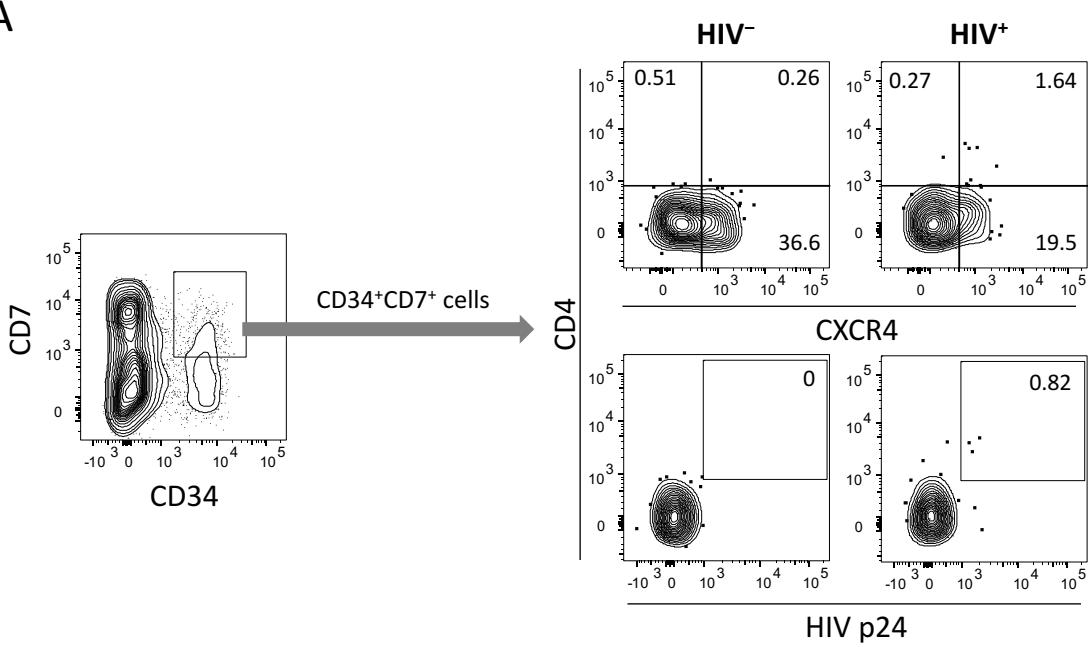

B

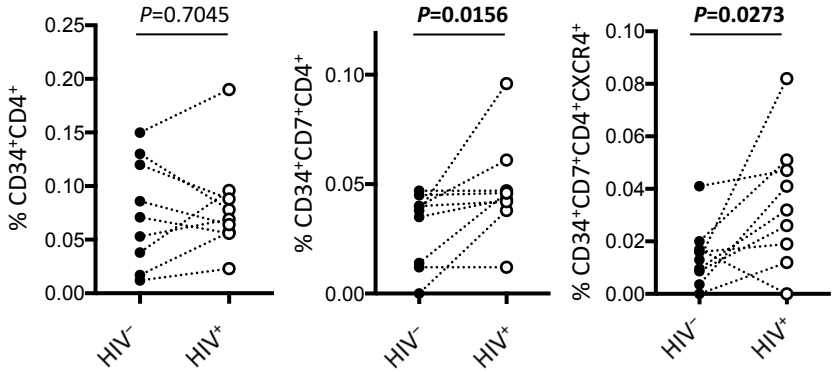

C

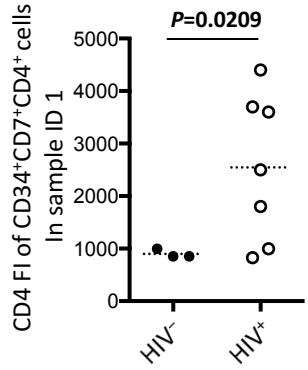

D

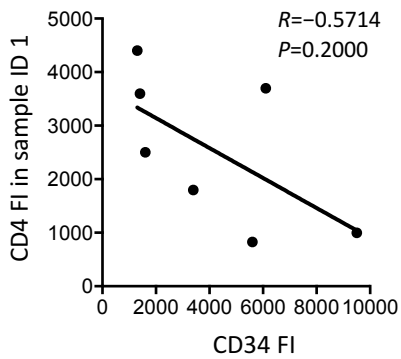

E

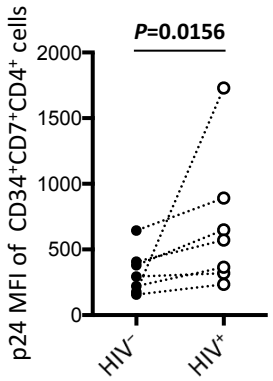

F

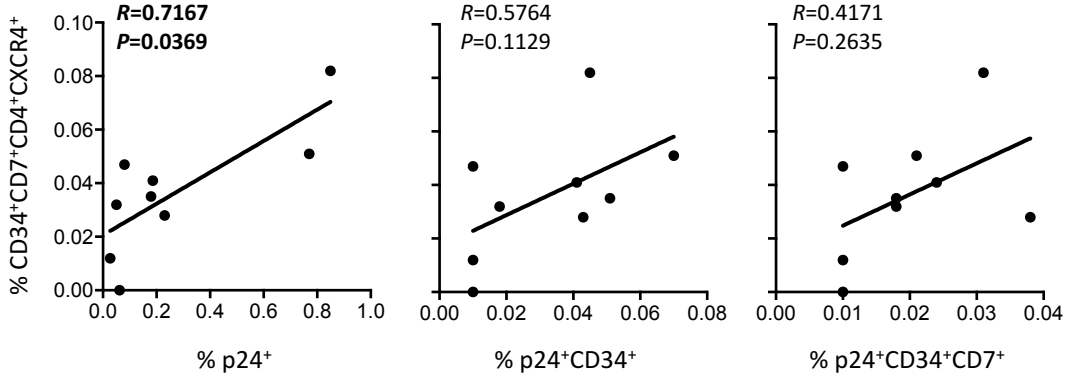

Figure S1

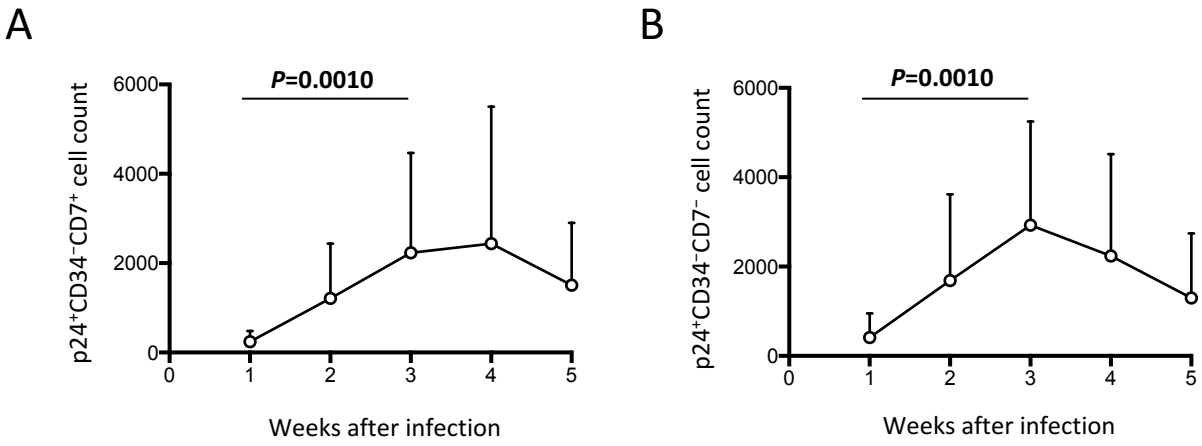

Figure S1. CD34⁻ cells were analyzed for expression of CD7 and intracellular HIV p24. (A) p24⁺CD34⁻CD7⁺ cell counts. (B) p24⁺CD34⁻CD7⁻ cell counts.

Figure S2

A

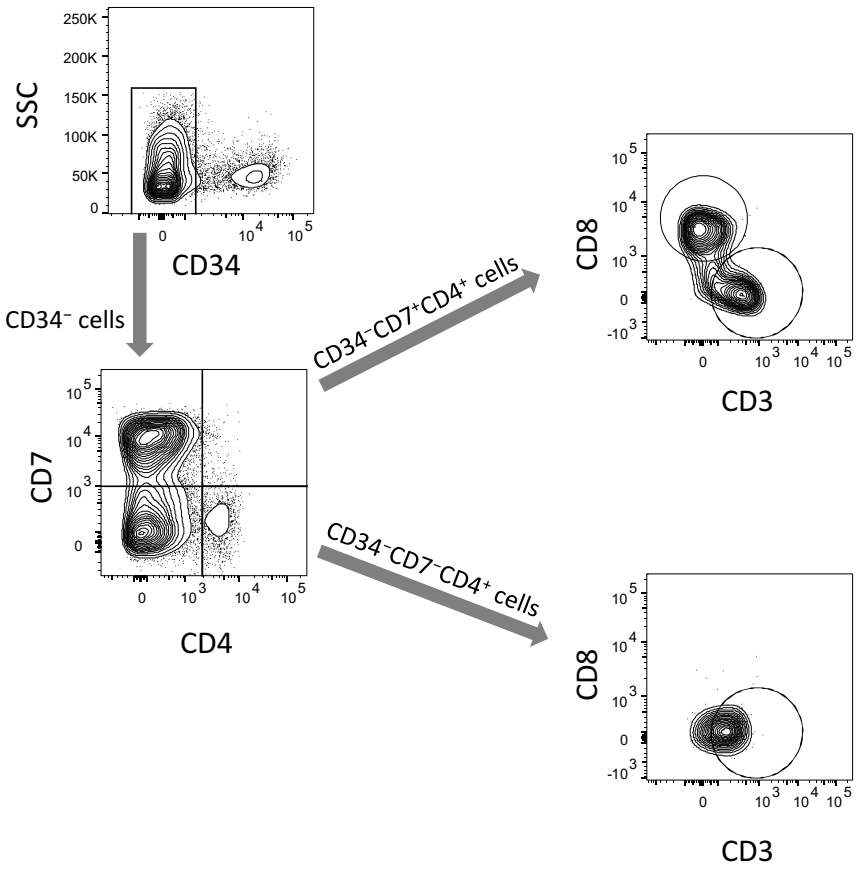

B

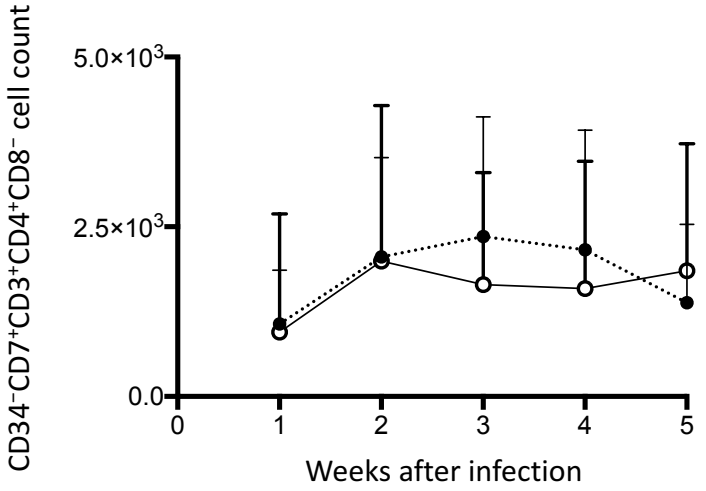

Figure S2. (A) Flow cytometry plots that complement Fig 2E. They show the phenotype analysis of $CD34^-CD4^+$ cells in an OP9-DL1 coculture. Representative plots are shown. Cord-derived $CD34^+$ cells were cocultured with OP9-DL1 for 4 weeks. Cells were collected and analyzed by flow cytometry. $CD34^-$ cells were gated by the expression of CD7 and CD4. $CD7^+CD4^+$ cells and $CD7^-CD4^+$ cells were further gated by the expression of CD8 and CD3. The analysis revealed that $CD7^+CD4^+$ cells contained different subsets including $CD3^-CD4^+CD8^+$ and $CD3^+CD4^+CD8^-$ cells, whereas $CD7^-CD4^+$ cells were mostly $CD3^+CD4^+CD8^-$ cells. These results indicate that CD4/CD8 double-positive thymocytes, $CD7^+$ CD4 T cells, and $CD7^-$ CD4 T cells were generated by the OP9-DL1 coculture of cord-derived $CD34^+$ cells. (B) $CD34^-CD7^+CD3^+CD4^+CD8^-$ cell counts.

Figure S3

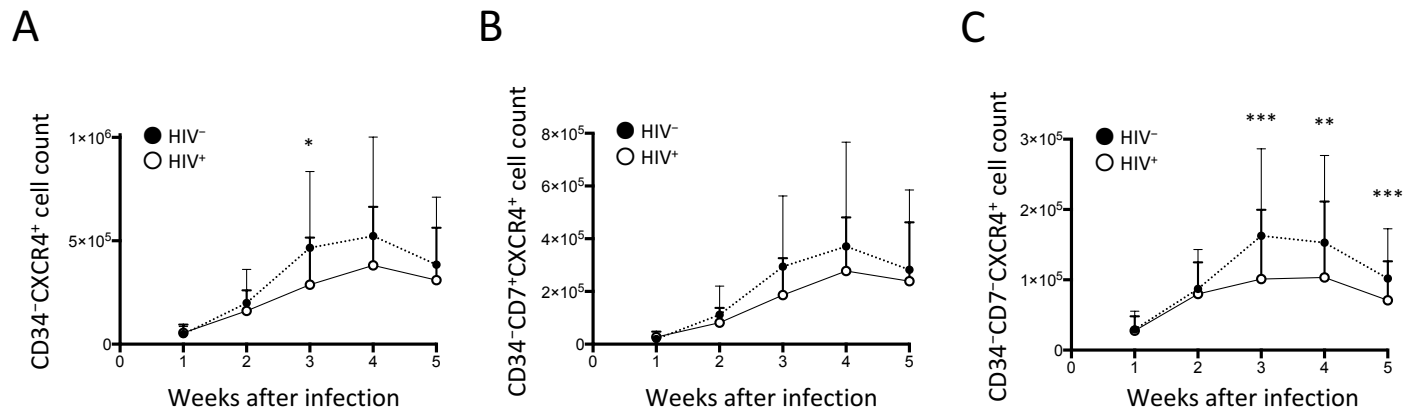

Figure S3. Part of the experiment 1 (long coculture) data. Phenotypes of $CD34^-$ cells in the OP9-DL1 cocultures HIV-1 infection were analyzed weekly from week 1 until week 5 post infection. Cell counts were compared with the samples without HIV-1 infection. These data complement Fig 2E-G. (A) $CD34^-CXCR4^+$ cell counts. (B) $CD34^-CD7^+CXCR4^+$ cell counts. (C) $CD34^-CD7^-CXCR4^+$ cell counts. Comparison was done by the Wilcoxon matched-pairs signed rank test. *: $P<0.05$, **: $P<0.01$, ***: $P<0.001$.

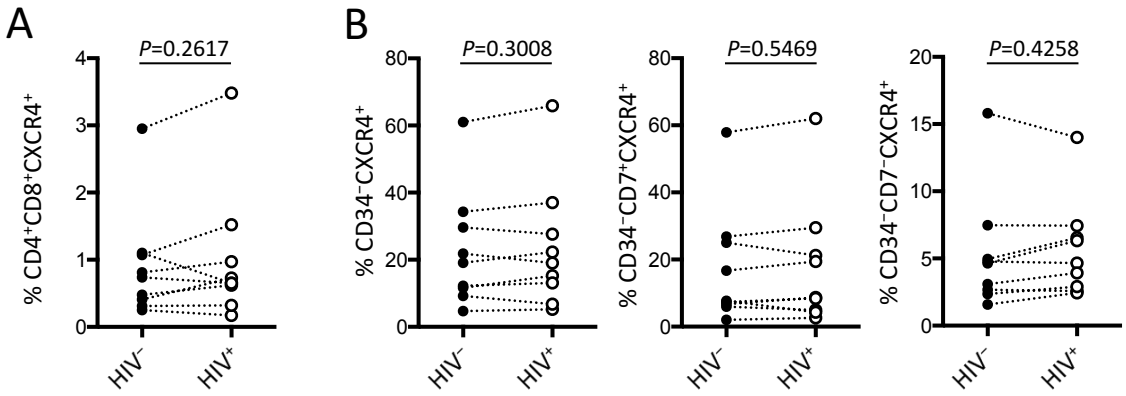

Figure S4. Part of the experiment 2 (short coculture) data. CXCR4$^+$ cells in different subsets were compared between HIV-infected and uninfected samples. (A) Frequencies of CD4$^+$CD8$^+$CXCR4$^+$ cells. (B) Frequencies of CD34$^-$CXCR4$^+$ cells (left), CD34$^-$CD7$^+$CXCR4$^+$ cells (middle), and CD34$^-$CD7$^-$CXCR4$^+$ cells (right). Comparison was done by the Wilcoxon matched-pairs signed rank test.

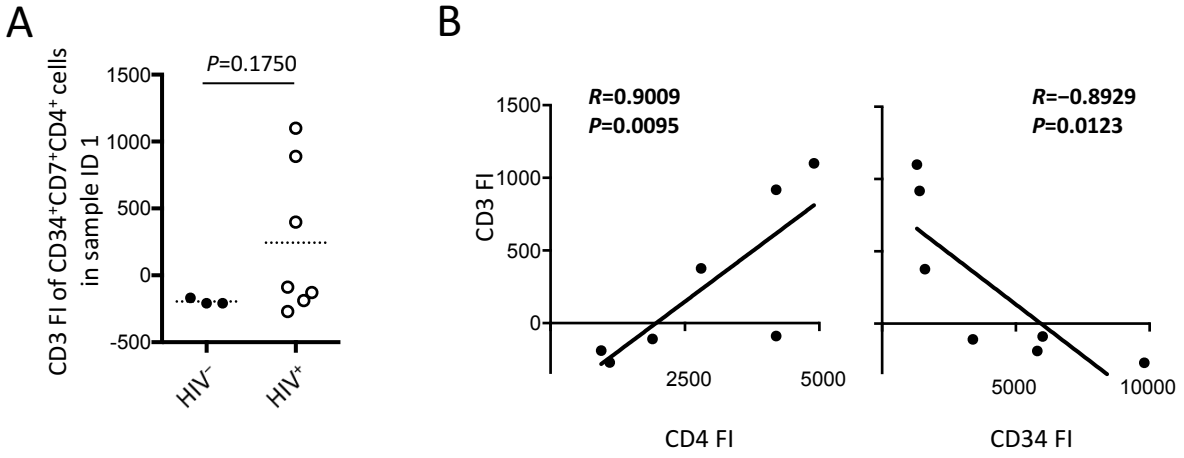

Figure S5. Part of the experiment 2 (short coculture) data. $CD34^+CD7^+CD4^+$ cells in sample ID 1 were further analyzed for CD3 fluorescence intensities (FIs). (A) Comparison of CD3 FIs between HIV-infected and uninfected samples. (B) Correlation analysis between CD3 FIs and CD4 (left) or CD34 (right) FIs. Spearman's rank correlation coefficients were calculated.